

NASA TM X-55750

# THE ORDERED MAGNETIC FIELD OF THE MAGNETOSHEATH

D. H. FAIRFIELD

N67-23320

FACILITY FORM 602

(ACCESSION NUMBER)

38

(PAGES)

TMX-55750

(NASA CR OR TMX OR AD NUMBER)

(THRU)

(CODE)

29

(CATEGORY)

APRIL 1967



— GODDARD SPACE FLIGHT CENTER —

GREENBELT, MARYLAND

THE ORDERED MAGNETIC FIELD OF THE MAGNETOSHEATH

by

D. H. Fairfield\*

NASA/Goddard Space Flight Center  
Greenbelt, Maryland

---

\*NAS-NASA Resident Research Associate at Goddard Space Flight Center,  
Greenbelt, Maryland

## ACKNOWLEDGEMENTS

The author wishes to thank Dr. N. F. Ness for the use of the IMP 2 data and for helpful suggestions during the course of this work. Useful discussions with Dr. H. E. Taylor and Mr. K. H. Schatten are also gratefully acknowledged.

## ABSTRACT

Simultaneous data from the IMP 1 and IMP 2 satellites in interplanetary space has revealed that magnetic field discontinuities seen at one satellite are subsequently seen at the other satellite with delay times which are consistent with the idea of magnetic fields frozen in the solar wind being convected away from the sun with the solar wind velocity. A one to one correspondence of discontinuities at the two satellites persists even when one of the satellites is in the magnetosheath, showing that interplanetary fields are convected into the magnetosheath. Analysis of the directional distribution of magnetosheath fields and their relation to simultaneously measured interplanetary fields shows that as the magnetosheath fields are convected around the magnetopause by the solar plasma they undergo distortion from their interplanetary values until they are aligned tangent to the magnetopause. A hydromagnetic interpretation of these results is that interplanetary field lines, after being convected through the earth's bow shock, become draped around the magnetosphere with the sense of the magnetosheath field being that of the incoming interplanetary field.

## 1. INTRODUCTION

Ever since its identification as the region between the closed geomagnetic field lines of the magnetosphere and the undisturbed interplanetary medium, the magnetosheath has been characterized as a region of fluctuating magnetic fields. (Sonett et al, 1960; Ness et al, 1964; Holzer et al, 1966; Siscoe et al, 1967). This is quite natural since magnetosheath magnetic field fluctuation with periods of order 1 to 100 seconds are in direct contrast to the much lower level of fluctuations in interplanetary space and, to a lesser extent, in the magnetosphere. The present paper investigates the average magnetic field upon which these fluctuations are superposed. It will be demonstrated that (1) the origin of the magnetosheath fields is the interplanetary field convected into the magnetosheath and (2) the average magnetosheath fields exhibit a high degree of spacial coherence due to a tendency of the fields to align themselves tangent to the magnetopause.

In this work measurements from the IMP 1 and IMP 2 satellite magnetic field experiment have been used. The two satellites were identically instrumented, each carrying two monoaxial fluxgate magnetometers which independently measured the vector magnetic fields as the satellite rotated. These vector measurements were obtained from 4.8 seconds of continuous data and the vector samples were obtained at intervals of 20.5 seconds. Details of the experiment and analysis procedures have been published previously (Ness, Searce and Seek, 1964; Fairfield and Ness, 1967).

IMP 2 was launched into a highly eccentric orbit on October 4, 1964 with its apogee at  $15.9 R_E$  near the earth-sun line. Subsequently the orbit moved toward the dawn meridian as the earth moved around the sun. The satellite penetrated the magnetopause on each of the first 70 orbits and thus IMP 2 was ideally suited for studying the magnetosheath in the dawn to noon region. Over 340 hours of magnetosheath data are available for a statistical study.

The IMP 1 satellite was launched into a highly eccentric orbit on November 27, 1963 with its apogee at  $31.3 R_E$  also near the earth-sun line. IMP 1 transmitted data continuously until May 1964 when battery failure and an unfavorable spin-axis sun angle forced the spacecraft into a non-operational undervoltage mode. After remaining inactive throughout the middle of 1964, the spacecraft spin-axis sun angle attained a value such that the spacecraft resumed operation, allowing acquisition of over 600 hours of data during November and early December 1964.

When IMP 1 resumed transmission almost one year after launch, its apogee was again near the earth-sun line, at a position almost two hours later in local time than that of IMP 2. The orbits of both satellites are shown projected in the solar ecliptic XY and XZ planes (X toward the sun, Y opposite the direction of the earth's orbital motion, and Z northward) in Figure 1, for the interval when most of the IMP 1 measurements used in this paper were made. Appropriate dates are shown on the orbits, and an average magnetosheath and shock are shown in the XY plane for reference. It can be seen from Figure 1 that IMP 1 will spend most of its time in the interplanetary medium while IMP 2 will spend a large portion of its time in the magnetosheath.

On those occasions when both spacecraft are simultaneously measuring the relatively steady fields of interplanetary space, we can compare measurements in order to check the accuracy of the measurement and/or field coherence over distances of the order of the separation between the satellites. Forty-eight intervals of approximately 5 minutes to 1 hour duration were available when both satellites were making measurements of relatively constant interplanetary fields. The average angular difference between the fields measured at the two satellites for these 48 cases was  $15.3^\circ$  with standard deviation  $7.1^\circ$ . The difference in magnitude measured at the two satellites was  $1.2\gamma$  (standard deviation  $\approx .9\gamma$ ) in total fields averaging  $8.7\gamma$ .

These differences are probably due partly to inaccuracies in the absolute values of the measurements on the two spacecraft. IMP 2 inaccuracies are undoubtedly the more important and have been estimated as  $\pm 10\%$  in magnitude and  $\pm 8^\circ$  in angle with the allowance that larger errors might occur in weak fields (Fairfield and Ness, 1967). A field direction dependence in the magnitude difference between the satellites suggests that IMP 2 zero levels may be in error by one or two gammas. IMP 1 accuracies were much better than IMP 2 during the first six months of the lifetime and appear not to have changed much by the fall of 1964; however, the effects of 6 months inoperation cannot be definitely assessed. Also, the lack of definitive information regarding the orientation of the IMP 1 spin axis in late 1964 necessitated use of the May value. This value has probably changed by a few degrees by November and would contribute to the angular discrepancy.

These differences in measurements between the satellites will not affect the conclusions of this paper and the small values permit some conclusions about the coherence of interplanetary magnetic fields over satellite separation distances of the order 10 earth radii. Even if the field differences at the two satellites are entirely instrumental, the differences quoted above may be taken as an upper limit to the coherence of interplanetary fields over these separation distances. The relatively good agreement between the satellites demonstrates that there is a high degree of coherence.



## 2. MAGNETIC FIELD CONVECTION

An example of simultaneous interplanetary measurements is shown in Figure 2. IMP 2 magnitude  $F$  and latitude and longitude angles  $\theta$  and  $\phi$  are plotted above the corresponding IMP 1 traces as a function of time. The fields are in solar magnetic or dipole coordinates (Fairfield and Ness, 1967) which are not importantly different from the solar ecliptic coordinates.

The time interval of 14:30 - 16:30 on November 15 occurred during a sudden commencement geomagnetic storm which began at 1009UT on November 15, 1964. This time is characterized by the largest interplanetary magnetic fields ( $\sim 20\gamma$ ) seen during the IMP 1 - IMP 2 lifetimes and is unique because of the large number of abrupt changes in field magnitude and angle. Five of these abrupt changes have been marked with vertical lines in Figure 2. The left hand line of the pair indicates the discontinuity at IMP 1 (average position  $X_{SE} = 20.0$ ,  $Y_{SE} = -7.0$ ,  $Z_{SE} = -4.5$  during this interval) while the right hand line indicates the discontinuity at IMP 2 (average position  $X_{SE} = 10.5$ ,  $Y_{SE} = 10.0$ ,  $Z_{SE} = -5.7$ ) occurring 3.3 minutes later. Eleven such clear discontinuities have been observed during the limited amount of time when both satellites are in the interplanetary medium. In all cases a discontinuity seen at one satellite is subsequently seen at the other satellite.

A velocity,  $V$ , may be calculated from these time delays by assuming a model where the discontinuity occurs at a surface approximated by a plane oriented perpendicular to the ecliptic plane and making an angle  $\alpha$  with the earth sun line. ( $|\alpha| < 90^\circ$  with  $\alpha$  positive in the quadrants containing the theoretical spiral field angle). The equation for  $V$  that follows from this model is

$$V = \frac{\Delta x + \Delta y \operatorname{ctn} \alpha}{\Delta t} \quad (1)$$

where  $\Delta x = x_1 - x_2$  and  $\Delta y = y_1 - y_2$  are the difference in solar ecliptic satellite positions, (subscript 1 designating the satellite nearest the sun) and  $\Delta t = t_1 - t_2$  is the time delay between observations of a discontinuity at the two satellites. The second term in the numerator of equation (1) is necessary since the satellites are not necessarily along a radial vector from the sun and the same volume element of plasma and field will not sweep past each satellite.

Three assumptions about  $\alpha$  have been considered: (1)  $\alpha = 90^\circ$  which implies that the discontinuity surface is perpendicular to the earth sun line such as might be produced by a spherical blast wave moving radially outward from the sun; (2)  $\operatorname{ctn} \alpha = \frac{V_s}{\Omega R}$  ( $\Omega$  the sun rotation period and  $R = 1$  astronomical unit) which is the theoretical equation relating the spiral angle of the interplanetary field to the solar wind velocity; and (3)  $\alpha = \phi_m$  where  $\phi_m$  is the angle of the line of intersection of the plane formed by the field vectors before and after the discontinuity and the solar ecliptic plane. This third calculation of  $\alpha$  assumes the existence of a tangential discontinuity where field vectors on either side of the discontinuity are parallel to one another and there is no field component perpendicular to the discontinuity.

The values of  $V$  calculated with these three assumptions are listed in Table 1 along with the times of the events, delay times and the several available direct measurements of the solar wind velocity,  $V_s$ , from the IMP 1 MIT plasma experiment (Binsack 1966). The values of  $V$  in

TABLE 1

Event No.	Date	IMP 1 Time	$\Delta t$ (sec) IMP 1—IMP 2	Calculated Velocity (Km/sec)			
				$\text{ctn } \alpha = \frac{V_s}{\sqrt{R}}$	$\alpha = 90^\circ$	$\alpha = \phi_m$	Measured $V_s$
1	Nov. 15	14:43:40 $\pm$ 0	205 $\pm$ 16	370	290	240	325
2	Nov. 15	15:21:54 $\pm$ 8	182 $\pm$ 16	430	330	360	325
3	Nov. 15	15:25:19 $\pm$ 50	201 $\pm$ 80				
4	Nov. 15	15:38:57 $\pm$ 8	202 $\pm$ 16	390	300	320	325
5	Nov. 15	15:55:30 $\pm$ 8	201 $\pm$ 30	390	310	330	322
6	Nov. 15	17:45:04 $\pm$ 8	184 $\pm$ 16	470	360	390	400
7	Nov. 15	18:05:12 $\pm$ 8	185 $\pm$ 60				
8	Nov. 15	19:27:39 $\pm$ 8	149 $\pm$ 60				
9	Nov. 17	5:15:21 $\pm$ 8	334 $\pm$ 30	480	370		
10	Nov. 17	7:32:43 $\pm$ 20	328 $\pm$ 50	470	360		
11	Nov. 17	9:10:30 $\pm$ 8	283 $\pm$ 16	560	410		

Table 1 will be due to (1) spacial discontinuities frozen into the highly conducting solar wind plasma moving radially outward from the sun with the solar wind velocity and (2) propagation of the discontinuity in the rest frame of the plasma with velocity  $V_p$ . The relatively good agreement of the  $V$  values in table 1 with the measured velocities  $V_s$  indicate that the  $V_s$  is more important than  $V_p$ . The small differences between measured  $V_s$  and calculated  $V$  may be due to either propagation effects, or to the limitations of the simple model. The differences in velocities  $V$  calculated by the three methods are such that no definitive statement can be made regarding preference of one over another. It is interesting to note, however, that all three calculated measurements reflect the 75 km/sec increase in measured  $V_s$  for event No. 6 relative to previous events. Additional events with complete plasma spectra are necessary to fully analyze the nature of these discontinuities. Until these data become available the discontinuities provide a unique means of tracing the flow of plasma from one location to another.

Since the interplanetary field is being convected into the bow shock front upstream from the earth, it would be expected that the field of the magnetosheath should be related to the incoming interplanetary field. This is confirmed by figure 3 which shows simultaneous measurements on November 16 when IMP 1 is in interplanetary space and IMP 2 is in the magnetosheath. There is an obvious correspondence in the direction of the interplanetary and magnetosheath fields even though the magnetosheath field exhibits fluctuations and its magnitude is approximately three times as large as the interplanetary magnitude. Two

more abrupt directional changes are seen at IMP 1 in the interplanetary medium and again they may be seen at IMP 2, even though the satellite is now within the magnetosheath. Delay times are longer here than in Figure 2 primarily because IMP 1 is now at apogee. Figure 3 is typical of a large quantity of data in the respect that sudden large directional changes in the interplanetary medium are always seen in the magnetosheath at a later time. The relation between the average fields at IMP 1 and the corresponding average fields at IMP 2 in the magnetosheath will be discussed in the next section.

### 3. ORIENTATION OF MAGNETOSHEATH MAGNETIC FIELDS

An investigation of the orientation of magnetosheath magnetic fields has been carried out using two different approaches. First a statistical analysis was performed on the more than 340 hours of IMP 2 magnetosheath data to determine the distribution of field orientations at different positions within the magnetosheath. Then a direct comparison was made between the smaller set of IMP 1 interplanetary measurements simultaneous with IMP 2 measurements in the magnetosheath. Both approaches show that the interplanetary field which is convected into the magnetosheath becomes draped around the magnetosphere with the magnetosheath fields tending to be tangent to the magnetopause.

The procedure used for studying IMP 2 field orientation was to divide a sphere representing a solar ecliptic coordinate system into 96 equal solid angles. Then the distribution of 5.46 minute average fields among these 96 equal solid angle regions was investigated for particular spacial regions. The division of the sphere was accomplished by first creating nine latitude regions bounded by the latitudes  $\pm 78.3^\circ$ ,  $\pm 54.3^\circ$ ,  $\pm 34.2^\circ$ ,  $\pm 10.8^\circ$ . The polar region above  $\pm 78.3^\circ$  each formed one region. The region between  $54.3^\circ$  and  $78.3^\circ$  was divided into eight intervals of  $45^\circ$  longitude, and lower latitude regions were divided into 12 or 18 intervals of  $30^\circ$  and  $20^\circ$  longitude.

The 96 regions are shown projected on a plane in Figure 4 where solar ecliptic longitude angle  $\phi$  is the abscissa and latitude  $\theta$  is the ordinate. The numbers in each region represent the number of 5.46-minute-average fields occurring in that region. Data used in Figure 4

are those taken during the first forty orbits between the magnetopause and approximately the center of the magnetosheath. This region will henceforth be referred to as the inner magnetosheath. Since the satellite spends more time near apogee in the outer magnetosheath, the 1100 5.46 minute averages in Figure 4 represent 30% of all magnetosheath measurements for this period.

The selection of magnetosheath data for use in this study has been carried out with particular care. On most orbits the magnetopause is clear and the magnetosheath data can be unambiguously isolated. On the few occasions when the magnetopause is not clear, data has been omitted rather than risk the inclusion of magnetosphere data. Several figures presented here will be restricted to the inner magnetosheath in order to more clearly represent the phenomena occurring. When the outer magnetosheath data is included the conclusions are not altered.

The outstanding feature of Figure 4 is the extremely anisotropic nature of the distribution. As many as 74 of the total of 1100 measurements occur in one region whereas 19 regions have no measurements at all. Ninety-five percent of the measurements occur in half the regions and 85% occur in one-third of the regions. This may be contrasted with the interplanetary medium where a similar analysis reveals that 76% occur in half the regions and 58% occur in one-third of the regions. If all data from throughout the magnetosheath during the first 40 orbits is used, the corresponding figures are 86% and 74%. This shows that the magnetosheath has a more anisotropic distribution than interplanetary space and in this sense the magnetosheath field is more ordered than

the interplanetary field. When the magnetosheath field is described as turbulent, it should be emphasized that the turbulence is superposed on an ordered field and it is generally of small amplitude compared to the ordered field. Clearly terms such as "chaotic" or "tangled" are inappropriate in a general characterization of magnetosheath magnetic fields.

After obtaining  $\theta$ - $\phi$  directional distributions such as Figure 4, contour lines were drawn illustrating the degree of anisotropy in the field direction. This type of presentation is shown in Figure 5. The area numbered one designates a region that is from one to three times more densely populated than it would be with an isotropic distribution, three designates three to five times isotropy, etc. Dotted contours enclose regions where no measurements at all occurred. The top panels in Figure 5 illustrate contours for IMP 2 interplanetary measurements and the remaining panels represent magnetosheath measurements.

IMP 2 made measurements during two solar rotations and detected four recurrent interplanetary sectors (Fairfield and Ness, 1967) where the interplanetary field pointed primarily either outward from or inward toward the sun (Ness and Wilcox, 1965). Left hand panels in Figure 5 illustrate measurements taken during positive sectors and right hand panels illustrate negative sectors. The top interplanetary panels show that the positive sector measurements are clustered near the theoretical spiral angle  $\phi = 135^\circ$  and the negative sector measurements near the opposite direction of  $\phi = 315^\circ$ . Measurements from the inner magnetosheath made during the same positive and negative sectors throughout the first forty orbits are shown in



the middle two panels. The peak of the distribution is now shifted from the interplanetary peak by approximately  $55^{\circ}$  to new values of  $75^{\circ}$  and  $255^{\circ}$ . These  $\phi$  directions are just those expected for fields in the equatorial plane aligned tangent to the magnetopause in the longitude region 0800-1200 local time covered by the first forty orbits. The bottom two panels illustrate data from orbits 54 to 72 covering the local range 0500 to 0700. Mariner IV measurements (Coleman et al, 1966) have been used to help define the interplanetary sectors during this interval. Near dawn the peak of the distribution is shifted another  $30^{\circ}$  from that of the centerpanels and again the tendency is for the fields to align themselves tangent to the magnetopause. The regions of zero field occurrence at the interplanetary spiral angle in the bottom panel illustrates how consistently the interplanetary field is distorted as it is convected inward toward the magnetopause.

In the positive sector magnetosheath panels of Figure 5 there is a tendency for southerly directed fields to have larger values of  $\phi$  and northerly fields smaller values. The opposite is true of negative sectors. This can be explained by considering the fact that inbound passes in the region of the inner magnetosheath occur near or slightly below the solar ecliptic plane while outbound passes occur at more southerly latitudes. In Figure 6 the outbound and the inbound passes through the inner magnetosheath during the first 40 orbits have been separated. The top panel inbound passes near the equatorial plane show good symmetry about a horizontal line while the bottom panel at lower latitudes exhibits the pronounced skewness described above.

This skewness is that expected for a distribution of field tangent to the theoretical magnetopause at southerly latitudes.

Comparison of simultaneous IMP 1 and IMP 2 measurements was accomplished by choosing intervals generally of 10 minutes to one hour duration during which the field was steady or only slowly varying. For 182 such intervals the average fields were calculated at IMP 1 in interplanetary space and IMP 2 in the magnetosheath. The time of the IMP 2 calculation was from five to ten minutes after that of IMP 1 to allow convection of the field from the IMP 1 region to that of IMP 2. Often discontinuities in the field were present to allow accurate calculation of this delay time. At other times the fields were varying slowly and an uncertainty of a few minutes would not be significant. Occasional times when the magnetosheath fields were undergoing particularly large and rapid fluctuations were omitted.

Next the field pairs with similar interplanetary values were grouped together and the magnetosheath vectors plotted at the position of measurement in the magnetosheath. In this manner the magnetosheath measurements made at various times (and therefore various positions) map the spacial dependence of the magnetosheath field for a given range of the interplanetary field values. All measurements when interplanetary fields are in the latitude range  $-30^{\circ} < \theta < 10^{\circ}$  are illustrated in Figure 7. In this figure vectors have been projected in the solar ecliptic XY plane and in each panel the sun is located at the bottom of the figure. Positive  $\theta$  values are designated by dashed vectors and average position for the shock and the magnetopause are sketched in for reference. Magnitudes have been normalized

to minimize the effects of the variation in interplanetary field magnitude. Normalized values are  $5.2 F_2/F_1$ , where the  $F_2$  represents the magnetosheath magnitude,  $F_1$  the interplanetary magnitude, and 5.2 is the average of all interplanetary values in gammas. Positions have been converted to the XY plane by rotation in a meridian plane.

The outstanding feature of Figure 7 is that for interplanetary fields  $0^\circ < \phi < 180^\circ$  (left hand panels) the magnetosheath fields tend to be tangent to the magnetopause pointing in one direction, while for  $180^\circ < \phi < 360^\circ$  (right hand panels) they are pointing in the opposite direction. The few exceptions such as near  $X=7$ ,  $Y=-11$  in the upper right hand panel have  $\phi$  angles of  $353^\circ$  and  $354^\circ$  and are thus near the division point of  $360^\circ$ .

Another presentation of the simultaneous measurements are shown in Figures 8 and 9. Here the interplanetary  $\phi$  value of IMP 1 is plotted in the abscissa and the magnetosheath  $\phi$  value at IMP 2 is the ordinate. If fields were not distorted as they convect into the magnetosheath, all points would lie along the  $45^\circ$  line. The larger dots in figure 8 represent measurements with  $-30^\circ < \theta < 30^\circ$  and the smaller dots  $30^\circ < \theta < 60^\circ$ . At large  $\theta$  values the angle  $\phi$  loses its significance and these cases are omitted. Figure 8 clearly demonstrates the preference of the magnetosheath for  $\phi$  values near  $50^\circ$  and  $230^\circ$  corresponding to field alignment tangent to the magnetopause. The abrupt transition determining which way the field will point occurs near  $180^\circ$  and  $360^\circ$ .

Figure 9 is similar to Figure 8 except that  $\theta$  at the two satellites is shown. The tendency is for  $\theta$  to be preserved better than  $\phi$  at the latitudes and longitudes sampled by IMP 2. There

also appears to be a tendency for the circles, which designate times with the interplanetary fields roughly tangent to the magnetosphere, to lie nearest the  $45^{\circ}$  line. When the interplanetary field is directed towards the sun and perpendicular to the magnetopause (squares) positive  $\theta$  tends to be increased in the magnetopause. When the field points away from the sun and perpendicular to the magnetopause the negative  $\theta$ 's tend to be decreased. This type of distortion appears to be that expected when field lines frozen in the solar plasma are distorted by plasma flowing around the magnetosphere.

An example of how distorted the interplanetary fields may become by the time they approach the magnetopause is illustrated in Figure 10. In this figure the interplanetary field at IMP 1 (solar ecliptic position  $X=24.9$   $Y=-18.5$ ,  $Z=2.2$ ) is shown along with the field of IMP 2 in solar magnetic coordinates. At approximately 0750 the outbound IMP 2 satellite penetrates the magnetopause at the dawn meridian (dashed line). The magnetosheath field near the magnetopause is very much different from the simultaneous interplanetary field, but the relation between the two fields is apparent from features such as the positive  $\theta$  region around 0845 which terminates with a discontinuity at IMP 1 at 0822 and at IMP 2 9 minutes later. Near 0850 there is another prominent feature in the  $\phi$  angle of each satellite. Before and after the high  $\phi$  region the interplanetary field direction is such that the direction of distorted fields at IMP 2 is about  $80^{\circ}$  different from the IMP 1 field. During the high  $\phi$  region, however, the interplanetary field is nearly parallel to the magnetopause and the field at IMP 1 is

only  $16^\circ$  different from that at IMP 2. At 0912 a rather small angle change occurs at IMP 1 yet it is of such a nature that it produces a larger change at IMP 2.

A schematic representation of magnetic fields in the vicinity of the earth is presented in Figure 11. The figure illustrates how field lines cross the shock with their direction in the magnetosheath being determined by whether the interplanetary field has a component pointing towards dawn or towards dusk. Comparing the upper portion of Figure 11 with the lower portion illustrates how a very small change in the  $\phi$  angle ( $40^\circ$  in the case shown) can completely alter the fields of the magnetosheath. The direction arrows on the fields shown can be reversed without altering the field topology. Figure 11 is very similar to Figure 21 of Spreiter et al (1966), who considered hydromagnetic flow around the magnetosphere.

The continuation of a field line in the top portion of Figure 11 from dawn all the way around the front of the magnetosphere and the apparent higher magnitudes on the dusk side are probably an exaggeration. It is more likely that the dusk portion of this field line which arrived at the magnetopause before the dawn portion is already moving around the magnetopause and is located above or below the magnetosphere. This type of motion suggests an increasing change in angle  $\theta$  with motion toward the dawn-dusk meridian.

#### 4. SUMMARY

Data from the IMP 1 and IMP 2 satellite have been used to study the magnetic field of the magnetosheath and its relation to that of interplanetary space. Simultaneous measurements of the interplanetary medium by the two satellites have revealed the presence of magnetic field discontinuities seen first at one satellite, then at the other, with delay times which are consistent with the concept of magnetic fields frozen in the solar wind being convected away from the sun with the solar wind velocity. When one satellite is in the interplanetary medium and the other in the magnetosheath, this one to one correspondence between field discontinuities observed at the two satellites persists, showing that interplanetary fields are convected into the magnetosheath. During convection past the magnetosphere the fields tend to become aligned tangent to the magnetopause so that when the characteristic magnetosheath fluctuations are averaged out, the magnetosheath field is even more ordered than the interplanetary field.

The incoming interplanetary fields undergo an increase in magnitude at the bow shock front which must be accompanied usually by a small angle change to make the normal component continuous across the shock. Subsequent convection into the magnetosheath is accompanied by further field distortion from the interplanetary value with the field lines tending to align themselves tangent to the magnetopause. Near the ecliptic plane this results in large changes in longitude angle  $\phi$  while the latitude angle  $\theta$  is better preserved. This field distortion can be interpreted as a draping of field lines around the magnetosphere with the direction of magnetosheath field lines being determined by the direction of the

incoming interplanetary field. For an interplanetary field near the equatorial plane with positive solar ecliptic y component, the magnetosheath field near the sunward magnetopause has a dawn-dusk direction. When the interplanetary y component reverses direction the magnetosheath field points in the opposite dusk-dawn direction. This means that positive interplanetary sectors with mostly positive y components will usually have a dawn to dusk direction orientation while negative sectors with negative-y interplanetary components will usually be directed the opposite way. Some positive sector fields will have negative y components (and negative sectors positive y components) so the specification of a sector does not absolutely specify the direction of fields in the magnetosheath.

The entire phenomenon is consistent with a hydromagnetic interpretation such as that of Spreiter (1966) whereby interplanetary field lines are convected into the magnetosheath where they become draped around the magnetopause. The magnetosheath field geometry is thus determined by the incoming interplanetary field and the pattern of plasma flow around the magnetosphere.

## FIGURE CAPTIONS

- Figure 1 Projection of the IMP 1 (solid lines) and IMP 2 (dashed lines) trajectories into the XY (top) and XZ (bottom) solar ecliptic planes. The time interval November 11-December 15 1964 is that when most of the IMP 1 measurements were made. The magnetopause and the bow shock are sketched in for reference.
- Figure 2 IMP 1 and IMP 2 simultaneous interplanetary measurements during a magnetic storm on November 15, 1964. Discontinuities are observed at both satellites and are marked with vertical lines.
- Figure 3 Simultaneous measurements with IMP 1 in the interplanetary medium and IMP 2 in the magnetosheath on November 16, 1964. A consistency of field direction at the two satellites are readily apparent as are the presence of discontinuities observed successively at the two spacecraft.
- Figure 4 Ninety-six equal area regions of the solar ecliptic sphere are shown projected on a plane. Numbers in each region designate the number of 5.46-minute-average field measurements occurring in each region.
- Figure 5 Contour diagrams representing the relative density of magnetic field pointing in the various  $\theta - \phi$  directions. Left hand panels represent measurements made during positive sectors and right hand panels represent measurements from negative sectors. The top two panels represent interplanetary measurements and the remaining panels represent measurements from the 0800-1200 and 0500-0700 local time regions of the inner



magnetosheath. The shifting peaks of the distribution represent alignment of the fields tangent to the magnetopause at the different longitudes.

Figure 6 Field direction contours for inbound equatorial passes through the inner magnetosheath (top) and outbound southerly latitude passes through the same region. The different shapes of the distribution reflect alignment of the field tangent to the magnetopause which is oriented differently in the different regions.

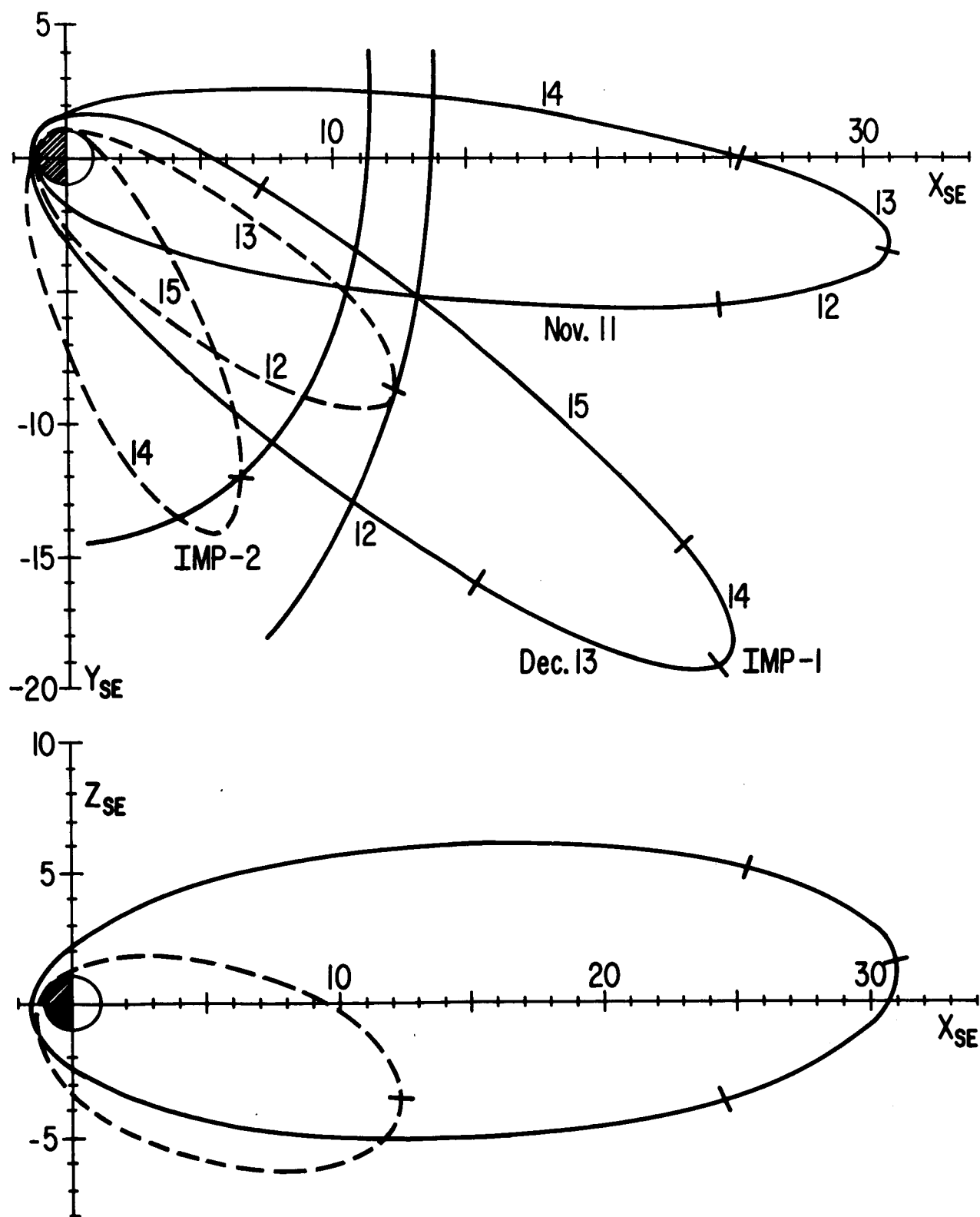
Figure 7 Projections of IMP 2 magnetosheath vectors in the XY plane are shown for 4 different directional groupings of the interplanetary field. For  $0 < \phi < 180$  the magnetosheath fields tend to point toward dusk and for  $180 < \phi < 360$  the fields point toward dawn.

Figure 8 Magnetosheath field longitude angle  $\phi_2$  is plotted versus the simultaneous interplanetary field longitude angle  $\phi_1$ . The grouping of magnetosheath fields near  $50^\circ$  and  $230^\circ$  reflects the tendency of fields to align themselves tangent to the magnetopause.

Figure 9 Magnetosheath field latitude angle  $\theta$  is plotted against the simultaneous interplanetary field latitude angle  $\theta_1$ . The interplanetary  $\theta$  value tend to be better preserved than the  $\phi$ , values of Figure 8.

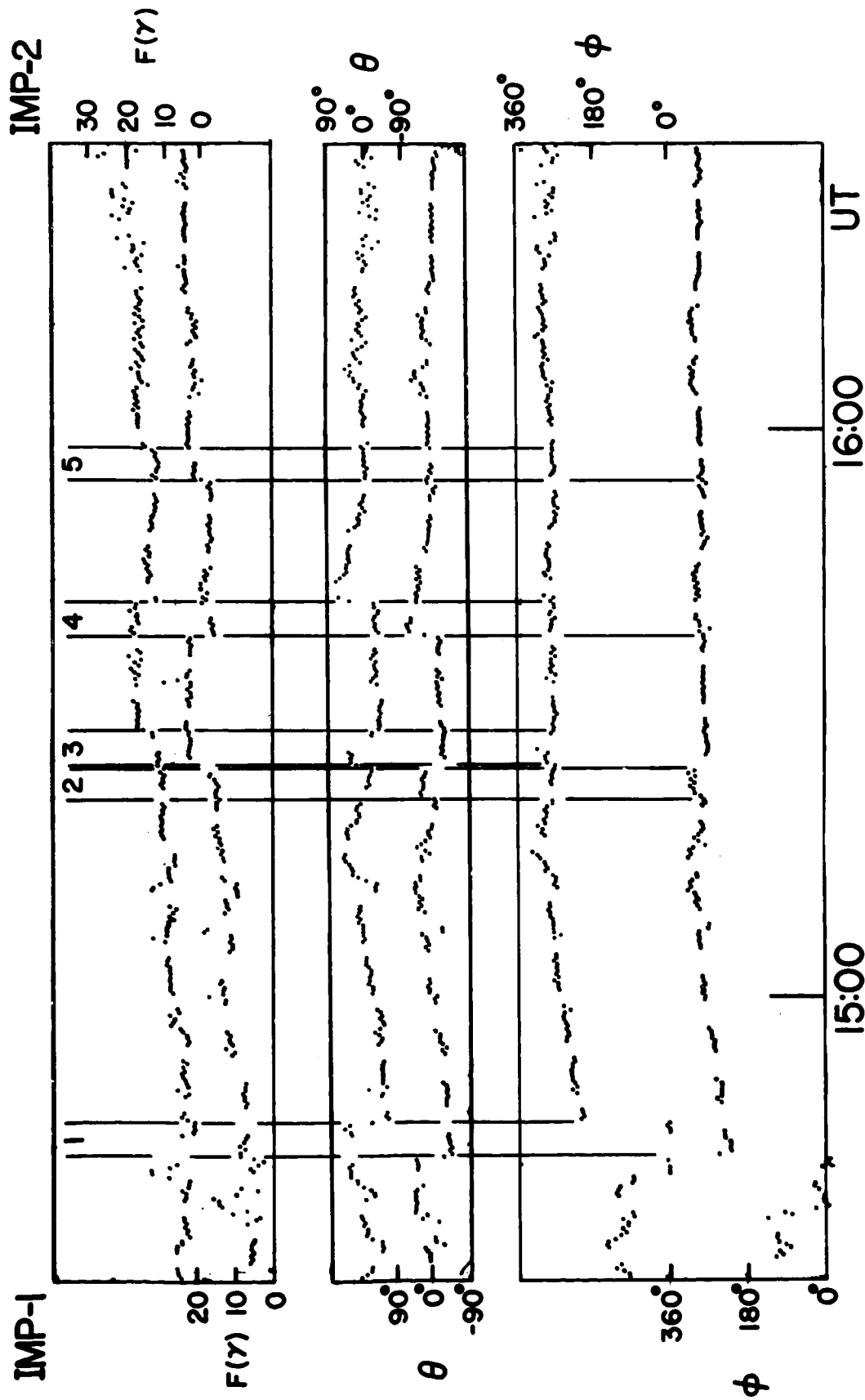
Figure 10 Simultaneous interplanetary IMP 1 fields and IMP 2 fields near the magnetopause at the dawn meridian plane. Correspondence in field direction angles at the two satellites is apparent although the IMP 2 magnetosheath field is considerably different from the interplanetary IMP 1 direction

Figure 11 A skematic drawing illustrating the draping of field lines around the magnetopause . A relatively small change in direction of the interplanetary field (top versus bottom) can produce a very drastic change in the magnetosheath field directions.



IMP TRAJECTORIES NOV. 11-DEC. 15, 1964

FIGURE 1



NOVEMBER 15, 1964

FIGURE 2

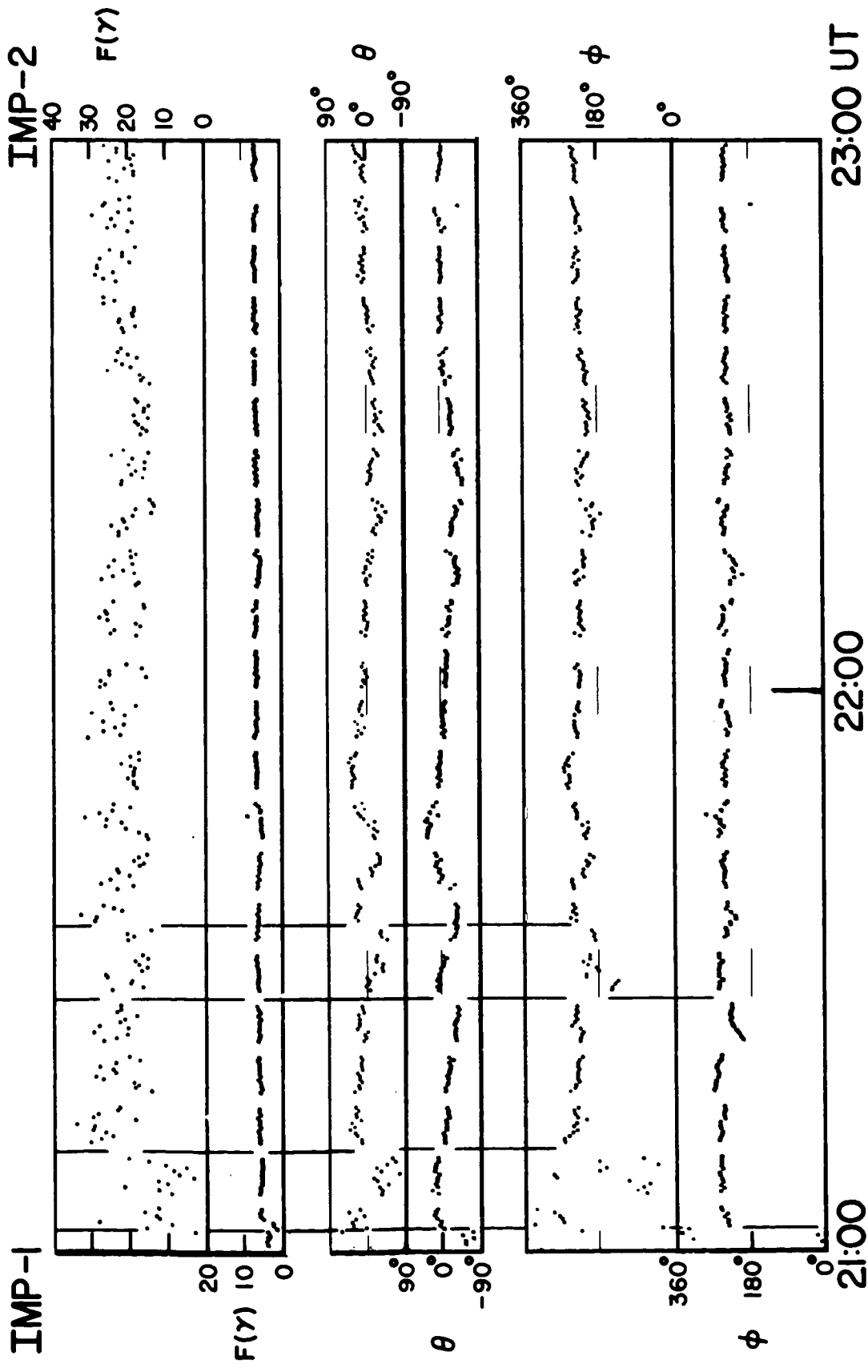


FIGURE 3

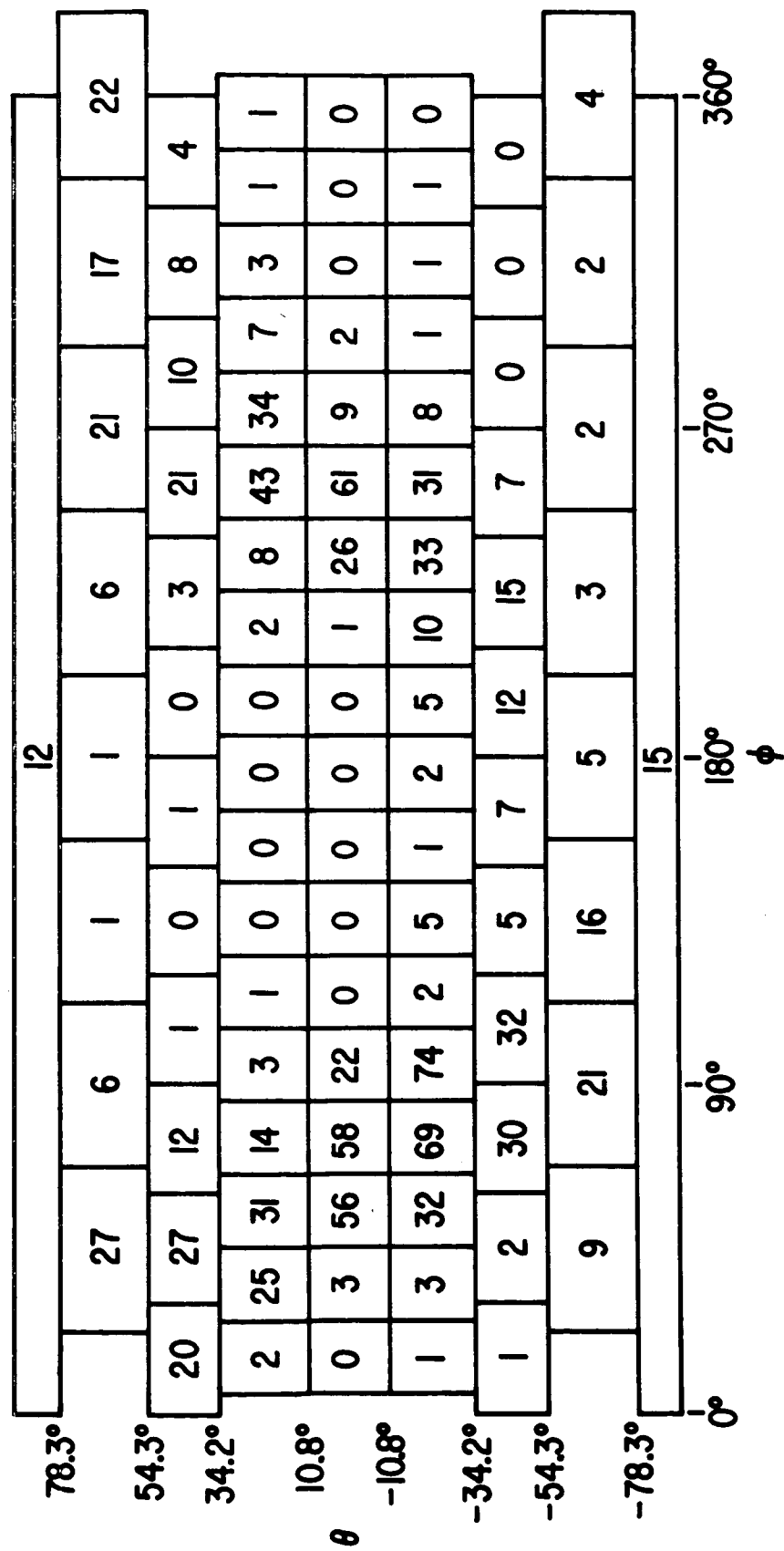


FIGURE 4

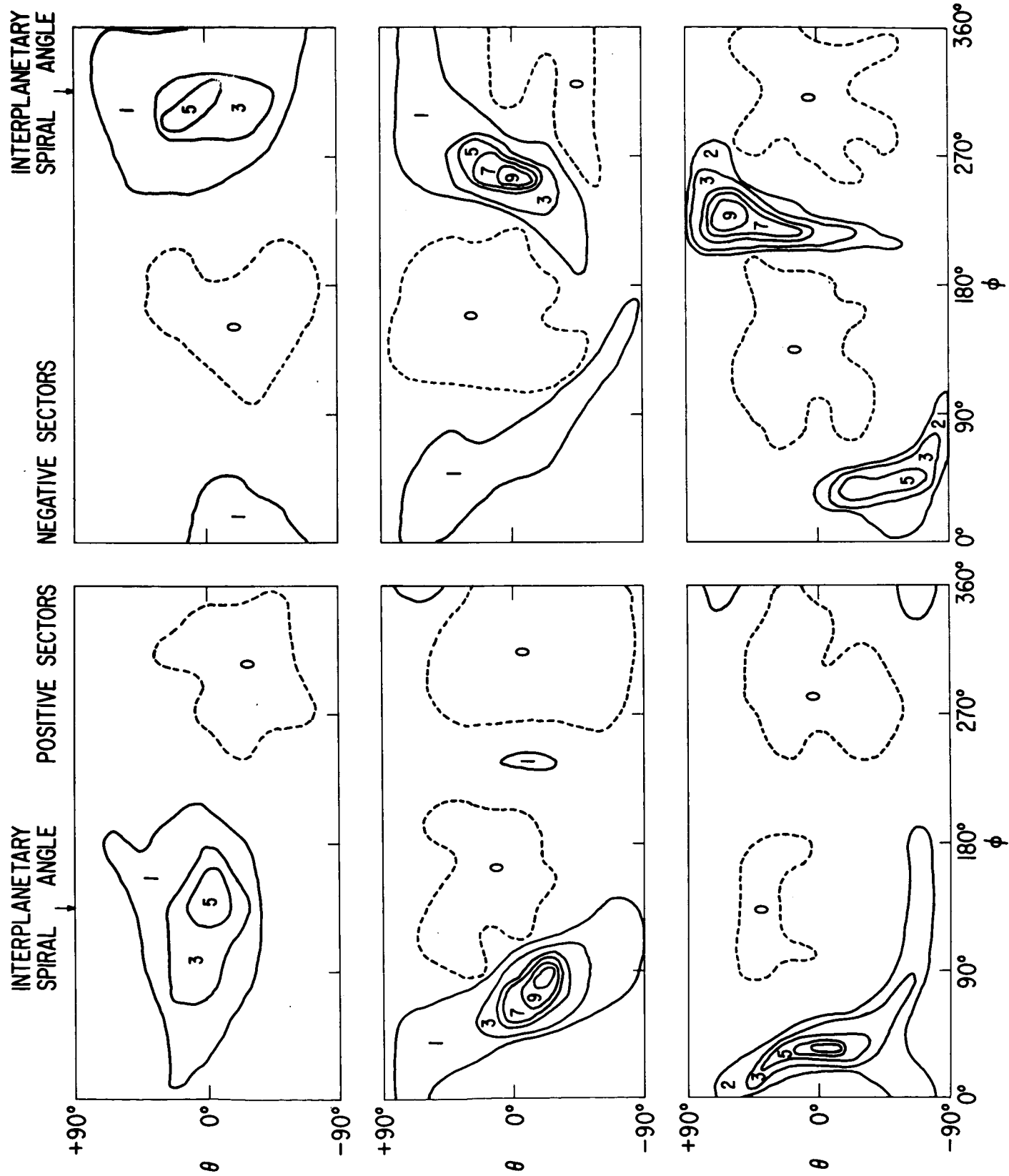


FIGURE 5

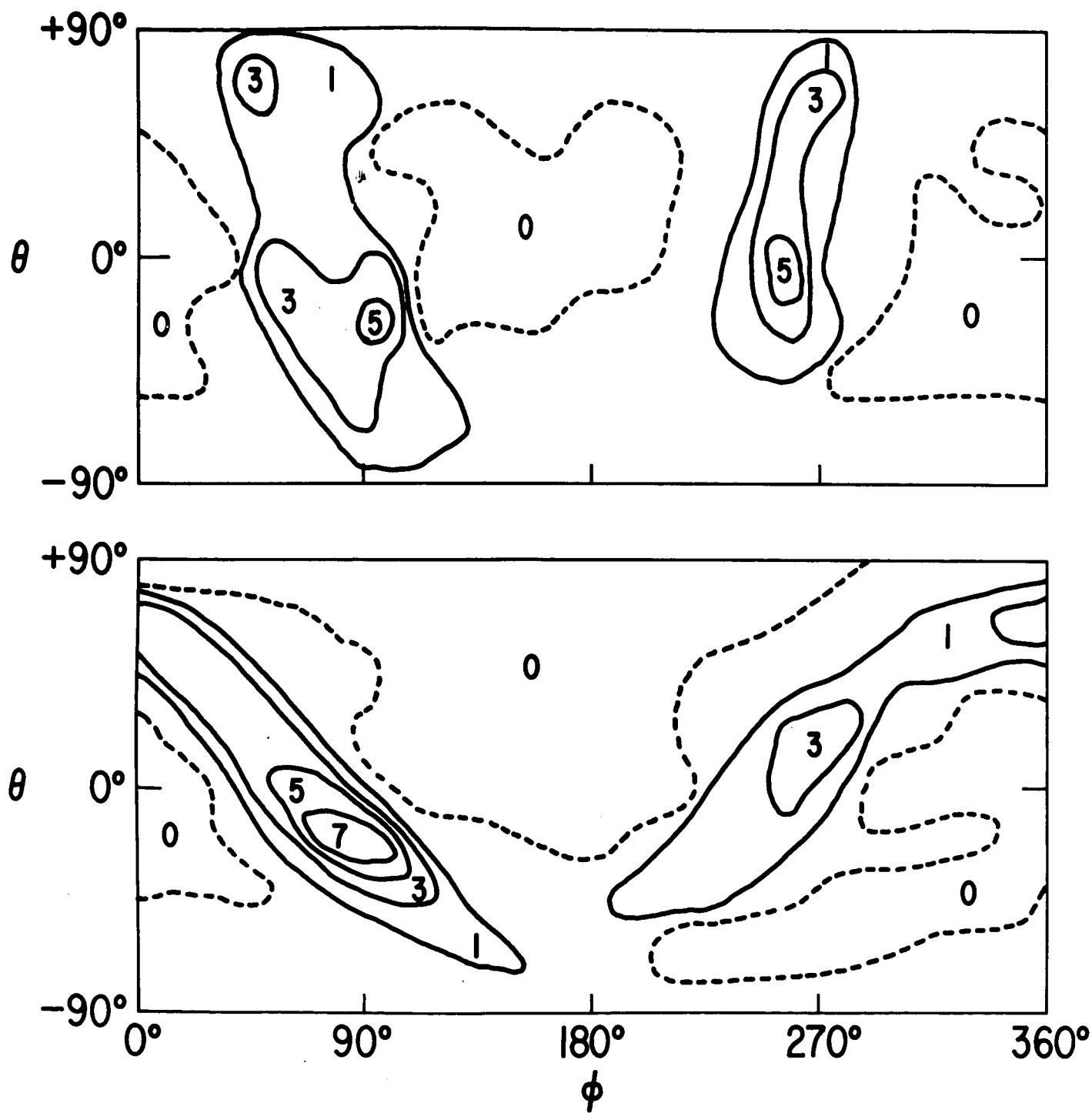


FIGURE 6



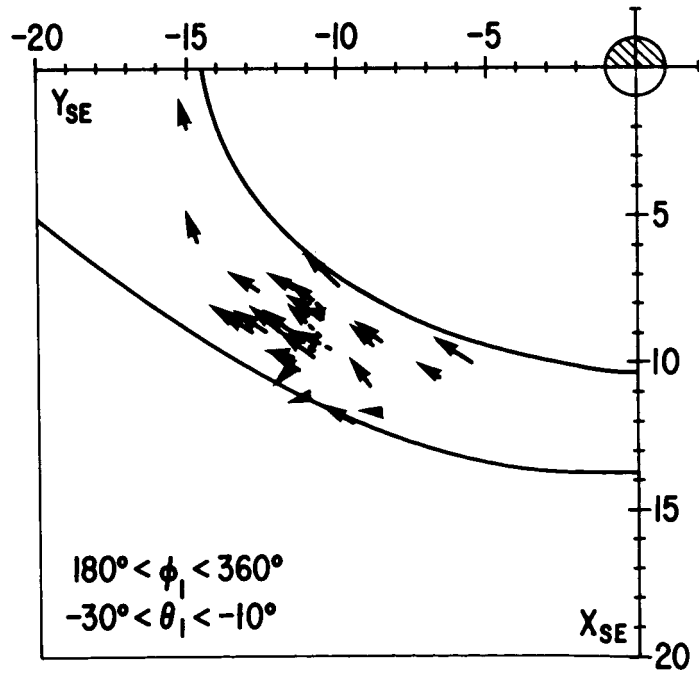
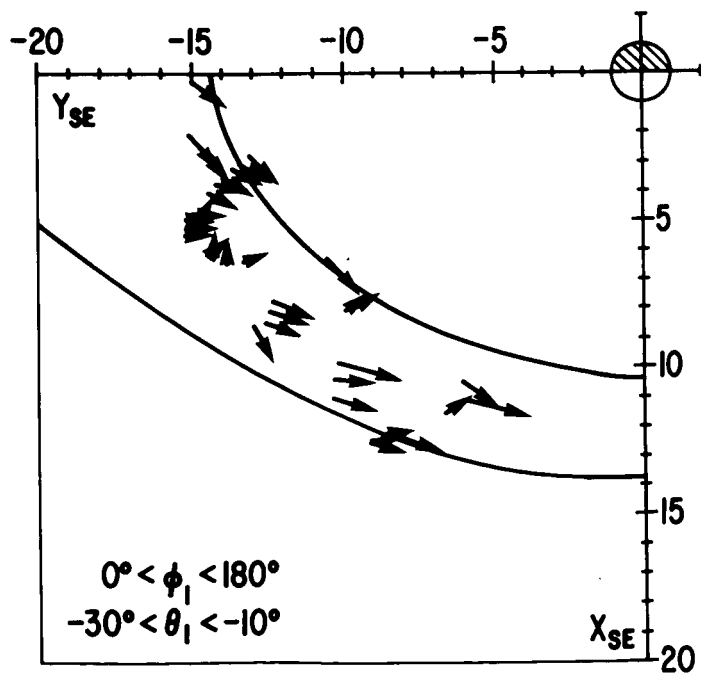
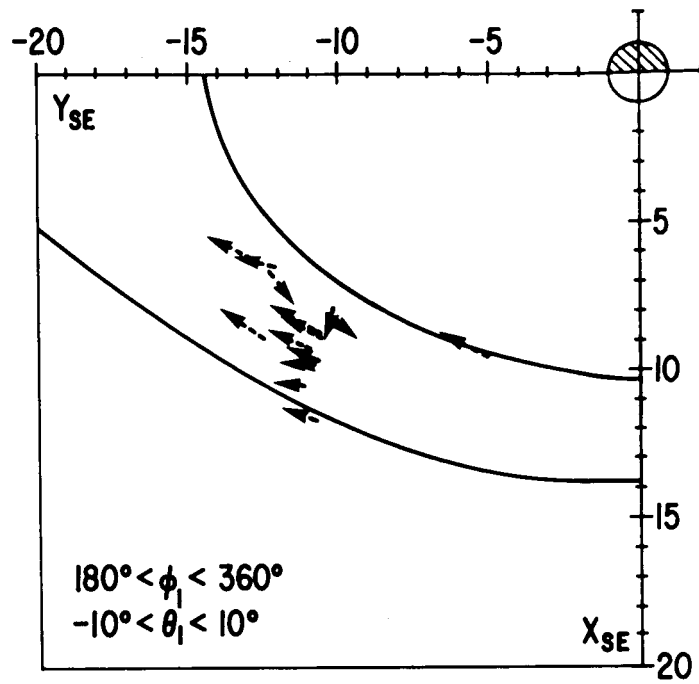
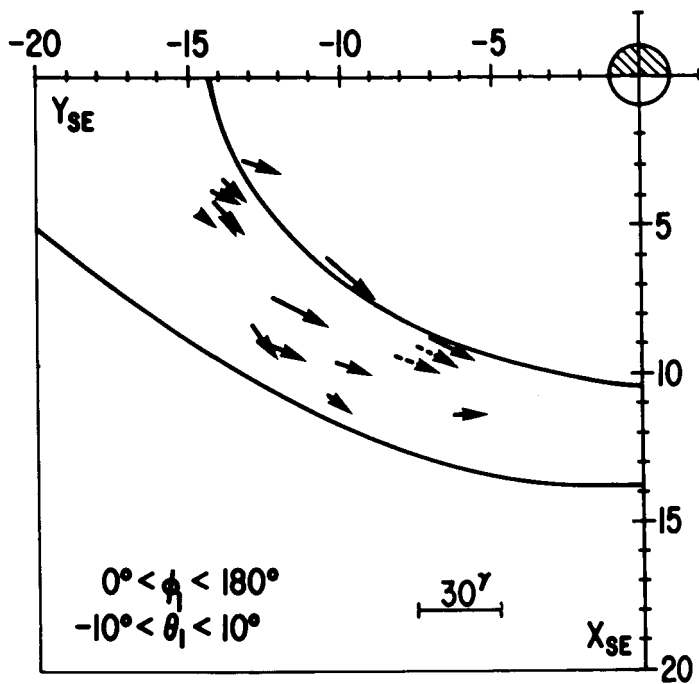


FIGURE 7

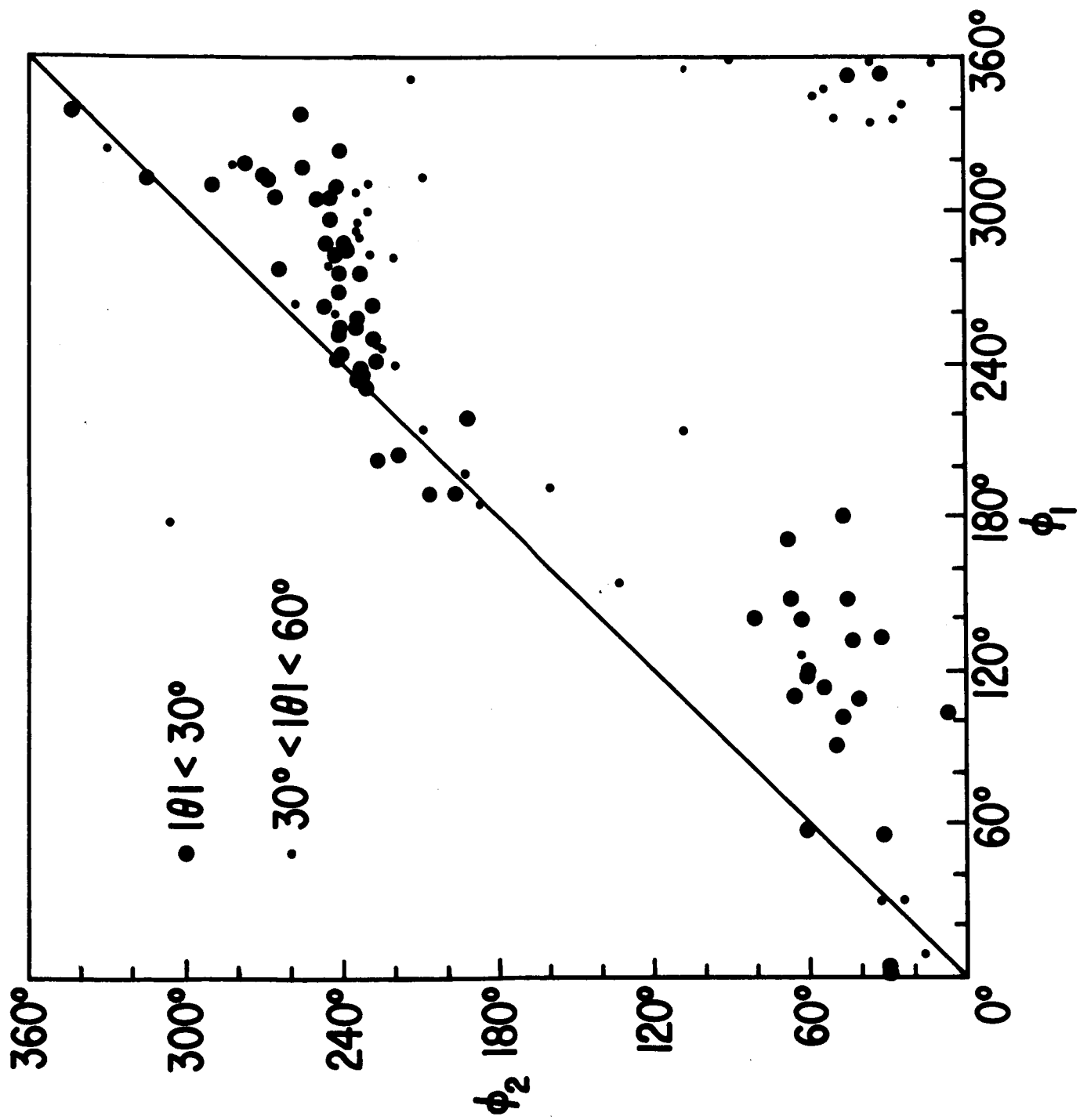


FIGURE 8

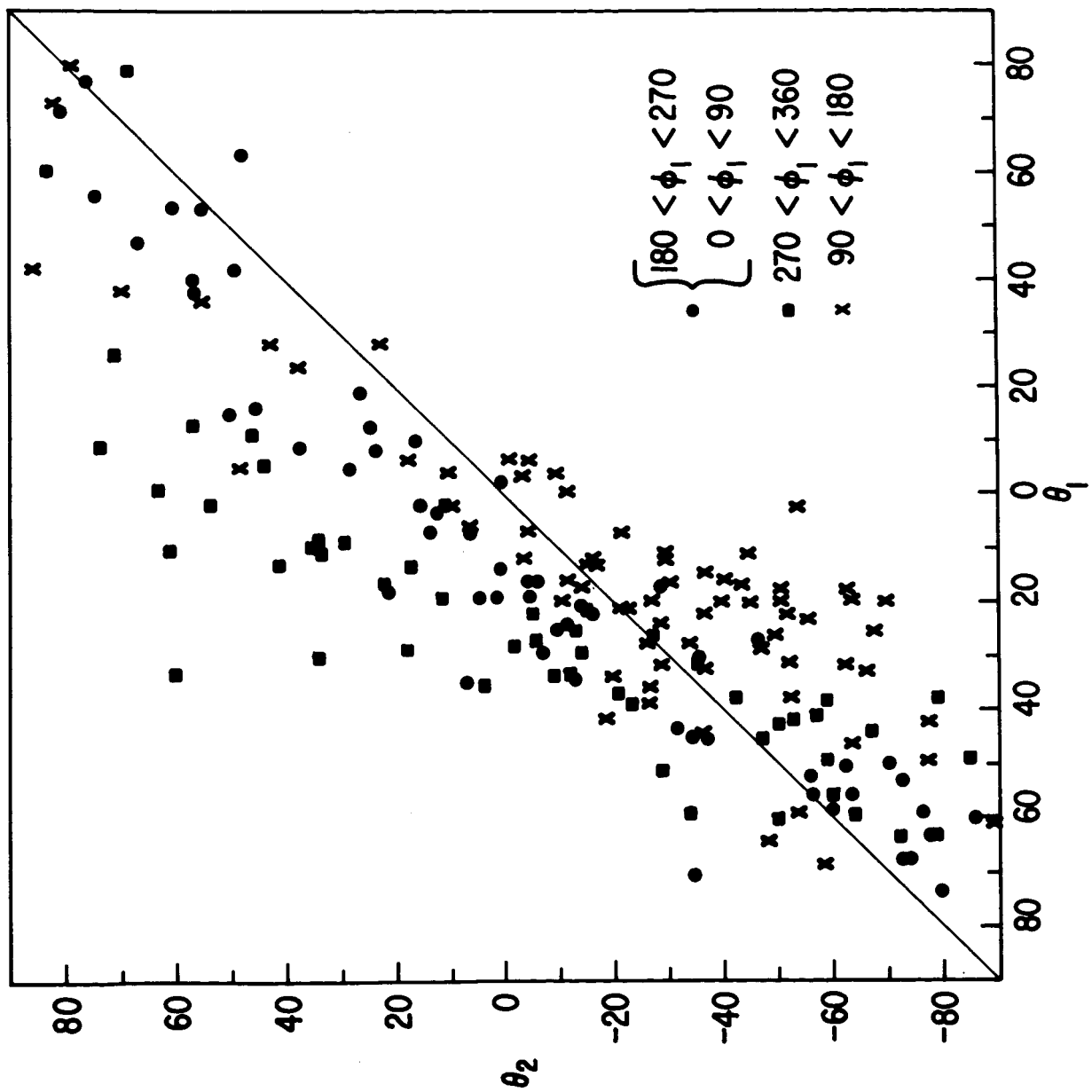


FIGURE 9

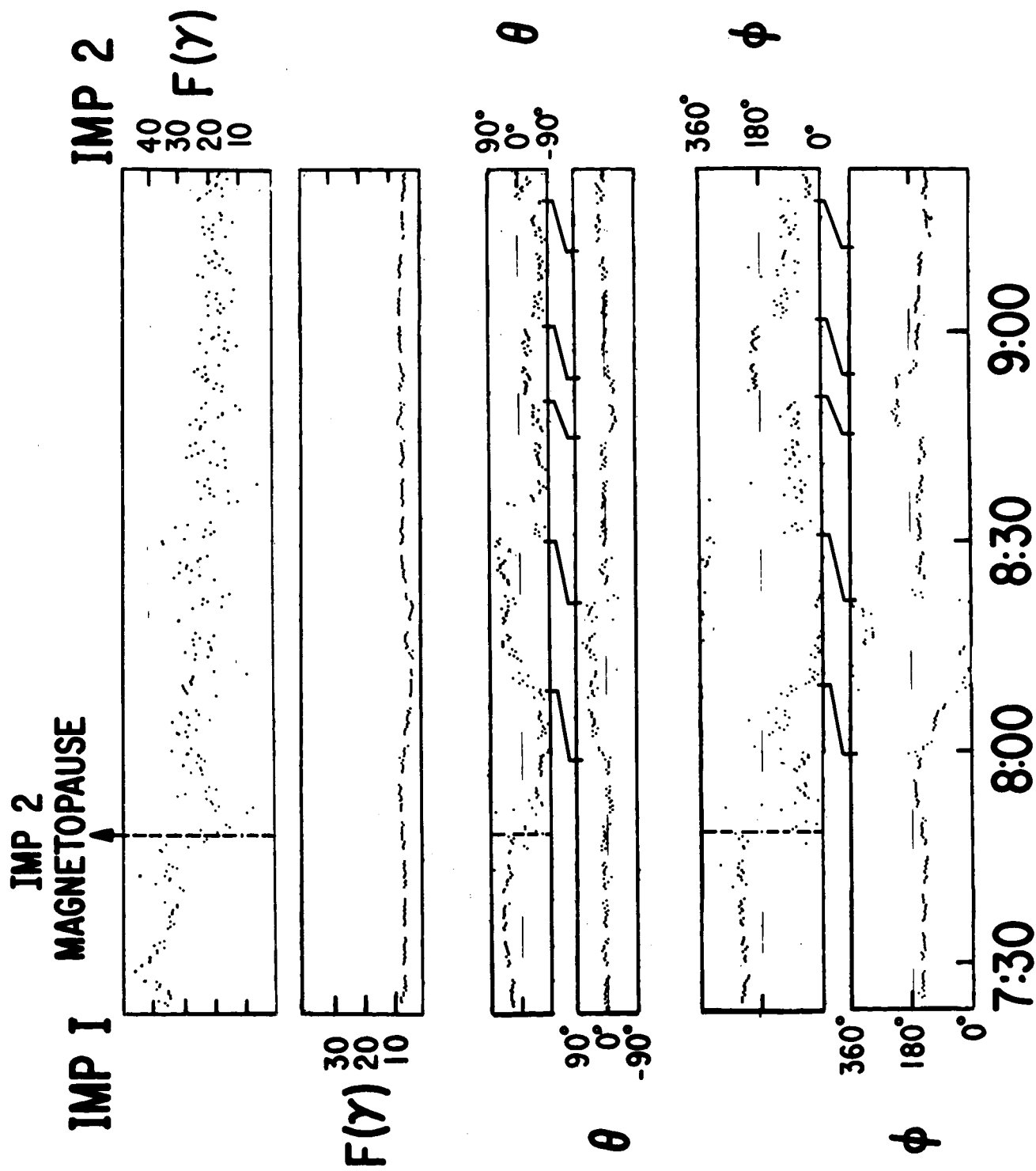


FIGURE 10

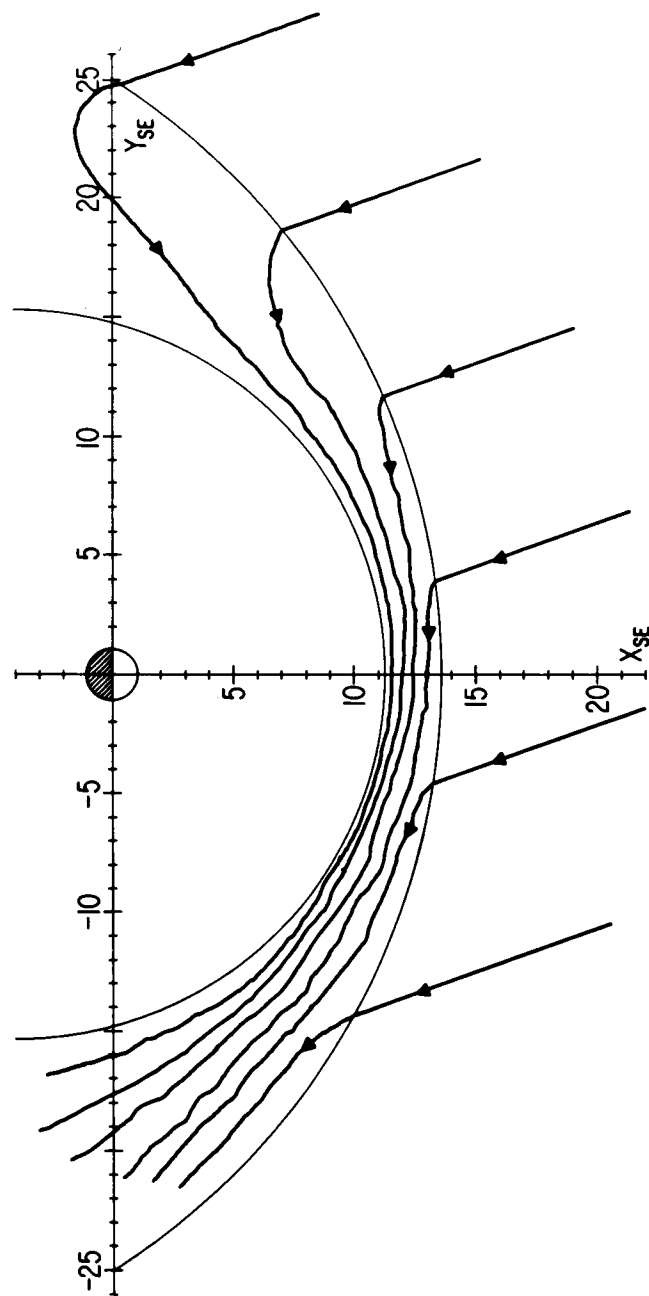
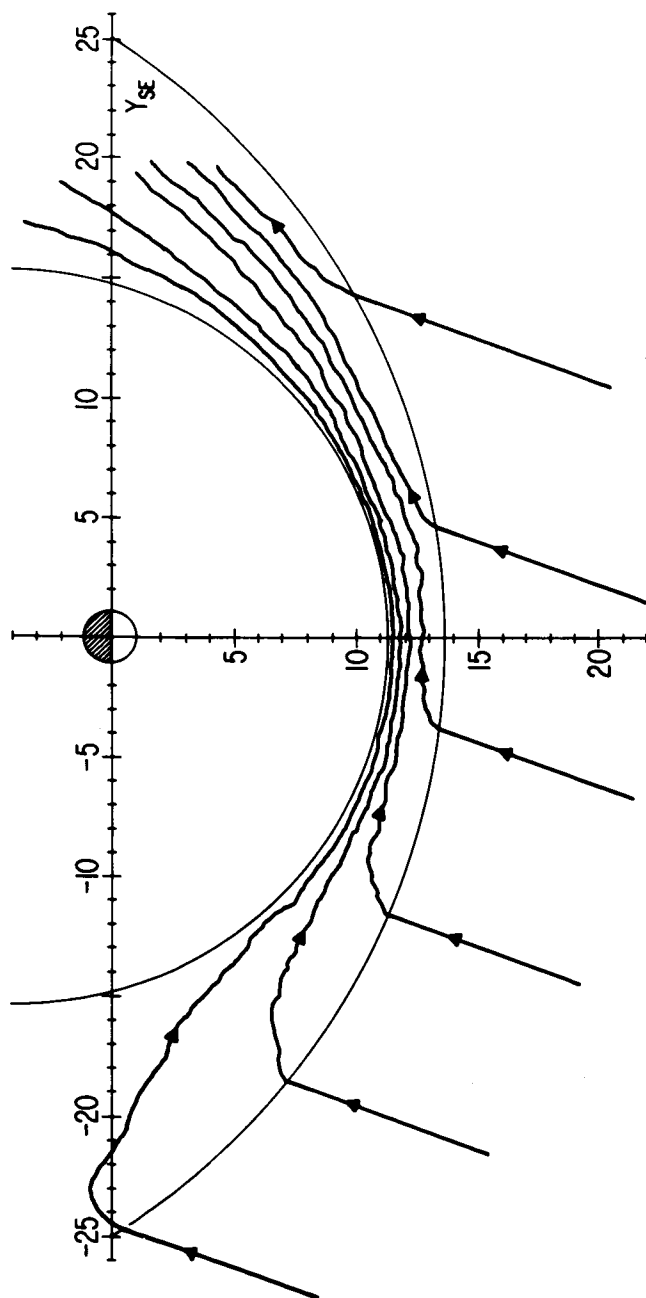


FIGURE 11

## REFERENCES

- Binsack, J. H., Plasma Studies with the IMP 2 Satellite, PhD Thesis MIT, 1966.
- Coleman, P. J., Leverett Davis, Jr., E. J. Smith, and D. E. Jones, Variations in the Polarity Distribution of the Interplanetary Magnetic Field, J. Geophys. Res. 71, 2831-2839, 1966.
- Fairfield, D. H., and N. F. Ness, Magnetic Field Measurements with the IMP 2 Satellite, J. Geophys. Res., May 1967.
- Holzer, Robert E., Malcolm G. McLeod, and Edward J. Smith, Preliminary Results from the OGO 1 Search Coil Magnetometer: Boundary Positions and Magnetic Noise Spectra, J. Geophys., Res., 71, 1481-1486, 1966.
- Ness, Norman F., and Clell S. Scarce and Joseph B. Seek, Initial Results of the IMP 1 Magnetic Field Experiment, J. Geophys. Res., 69, 3531-3531, 1964.
- Ness, Norman F. and John M. Wilcox, Sector Structure of the Quiet Interplanetary Magnetic Field, Science, 148, 1592-1592, 1965.
- Siscoe, G. L., L. Davis, Jr., E. J. Smith, P. J. Coleman, Jr., and D. E. Jones, Magnetic Fluctuations in the Magnetosheath: Mariner 4, J. Geophys. Res., 72, 1-17, 1967.
- Sonett, C. P., D. L. Judge, A. R. Sims, and J. M. Kelso, A Radial Rocket Survey of the Distant Geomagnetic Field, J. Geophys. Res., 65, 55-68, 1960.
- Spreiter, John R., Audrey L. Summers, and Alberta Y. Alksne, Hydromagnetic Flow Around the Magnetosphere, Planet, Space Sci. 14, 223-263, 1966.